

ORIGINAL ARTICLE

Morphology of nanoimprinted polyimide films fabricated via a controlled thermal history

Sudu Siqing¹, Hui Wu² and Atsushi Takahara^{1,2}

Fabricating nanopatterns on polyimide (PI) films directly by nanoimprint lithography (NIL) is difficult owing to the high glass transition temperature (T_g). In this study, a nanopatterned PI film was successfully obtained by nanoimprinting poly(amic acid) (PAA) film and curing it afterward. Differential scanning calorimetry, thermogravimetry and dynamic mechanical analysis were carried out to study the state of thermal molecular motion in PAA thick films that have the same content of residual solvent as the PAA thin films used in NIL. The thermal and dynamic mechanical behaviors of PI thick films were studied for comparison. An appropriate nanoimprinting process was proposed based on an understanding of the thermal and dynamic mechanical properties of PAA and PI films. Atomic force microscopy showed that the line pattern was transferred without distortion from the PAA film to the PI film, even though a larger shrinkage took place during the hard baking.

Polymer Journal (2012) 44, 1036–1041; doi:10.1038/pj.2012.53; published online 18 April 2012

Keywords: dynamic mechanical behavior; hard baking; nanoimprint lithography; poly(amic acid); polyimide

INTRODUCTION

Polyimide (PI) is one of the most promising thermally stable engineering plastics. PI has excellent properties, such as low toxicity, chemical resistance, strong mechanical strength, good heat resistance, high stability in a vacuum, anti-radiation, a low dielectric constant and good optical properties.^{1,2} On the basis of these advantages, PI has been widely used in space flight, printed circuits, liquid crystal displays and other high-tech fields.^{3–7} Recently, the nanotextures fabricated on PI films have been fabricated have been used in various applications, such as microelectronic devices,⁶ biological applications⁷ and alignment layers for advanced liquid crystal displays.^{4–6} To apply high-performance patterned PI films to high-tech fields, it is crucial to develop novel methods to fabricate line patterns to replace the traditional rubbing method because the traditional rubbing method would contaminate the surface and easily damage the device underneath.

In the past decade, nanopatterned polymer surfaces with various functionalities have been studied in depth.⁸ The patterning of surfaces can be completed by several popular methods. Photolithography has been widely used; however, the cost of production is very high.⁹ Electron-beam lithography and scanning-probe nanolithography are often utilized to generate very small features, but their development into practical commercial methods for low-cost, high-volume processing still requires great ingenuity.^{10,11} Surface-modified lithography may contaminate the sample and limit the selectivity between the polymer and self-assembled monolayer.¹² Nanoimprint lithography (NIL), which is convenient, effective and of low cost, has been demonstrated to be one of the promising approaches for the fabrication of high-quality polymer micro/nanostructures.^{13–15}

In general, NIL requires high pressure to overcome the hardness and viscosity of polymeric resistance and to create a relief pattern via physical deformation. When applying nanoimprinting pressure, the polymer film should be heated above the glass transition temperature (T_g) to make the polymer flow into a patterned mold. However, PIs have a high T_g (>300 °C), which limits the application of the microscale/nanoscale-patterned PIs as LC alignment layers in industry.^{4–6} Three approaches using NIL to pattern PI films have been developed:¹⁶ imprint at the uncured soft state and cure the film afterward; imprint another low T_g polymer, then transfer the pattern into PI by reactive-ion etching; and direct imprint into PI at a temperature higher than its T_g . The first approach is relatively simple and fast, but some residual solvent and water may cause outgassing when the PI is subjected to temperatures well above 200 °C for a prolonged period of time. The second approach is more complex, and the dry etching may increase the surface roughness, which would lead to more loss for optical waveguides. The third approach requires high temperatures, 350–550 °C depending on the type of PI. Comparing the above three approaches, we prefer the first method because it is simple and the imprinting temperature is lower. In addition, this approach is more suitable for massive fabrication in industry. The current problems are to keep the imprinting temperature <200 °C to avoid outgassing and the distortion of the pattern due to film shrinkage during hard baking.

The success of the NIL process relies on the imprinting conditions of pressure, temperature and time. To obtain appropriate conditions for NIL, it is necessary to understand the thermal and dynamic mechanical behavior of the polymer. In this study, a nanoimprinting

¹Graduate School of Engineering, Kyushu University, Fukuoka, Japan and ²Institute for Materials Chemistry and Engineering, Kyushu University, Fukuoka, Japan
Correspondence: Professor A Takahara, Institute for Materials Chemistry and Engineering, Kyushu University, 744 Motooka, Nishi-ku, Fukuoka 819-0395, Japan.
E-mail: takahara@cstf.kyushu-u.ac.jp

Received 2 December 2011; revised 6 February 2012; accepted 19 February 2012; published online 18 April 2012

condition for PI was proposed through the consideration of differential scanning calorimetry (DSC), thermogravimetric analysis (TGA) and dynamic mechanical analysis (DMA) results for poly(amic acid) (PAA) films and PI films. Atomic force microscopy (AFM) was applied to characterize the nanoimprinted structure before and after hard baking.

EXPERIMENTAL PROCEDURE

Preparation of PAA solution

Oxydianiline (Wako Chemicals Co., Osaka, Japan), pyromellitic dianhydride (Wako Chemicals Co.) and *N*-methyl-2-pyrrolidone (NMP; Wako Chemicals Co.) were chosen as reactants because they are the most popular in the industry (Kapton film, DuPont, Circleville, OH, USA) for a variety of applications. The PAA NMP solution was prepared by solution condensation polymerization at ambient temperature and at a composition of 14.5 wt% by solvent. Pyromellitic dianhydride (5.453 g, 0.025 mol) was added increasingly to a stirred oxydianiline (5.060 g, 0.025 mol) NMP solution in an ice bath. After PDMA was added to the solution, the ice bath was removed and the solution continued to be stirred for 6 h. An oil bath was used to heat the solution to 70 °C for 30 min then cooled down to room temperature naturally. The PAA solution was sealed and preserved in a 3 °C refrigerator for later use. Scheme 1a shows the synthesis of PAA and the imidization reaction.

Preparation of a PAA thick film for measurement of DSC, TG and DMA

A PAA thick film was prepared by coating PAA NMP solution (7.3 wt%) on glass for the study of the thermal and dynamic mechanical properties. The film with the glass substrate was dried at 30 °C for 7 days. This low temperature and long time was used to obtain a film with a smooth surface. After drying, the PAA film with a thickness of ca. 61 μm was peeled from the substrate.

Preparation of PAA thin films for NIL

The silicon (Si) wafers were cleaned in a fresh piranha solution (a mixture of 98% H₂SO₄ and 30% H₂O₂ with a volume ratio of 7:3) at 90 °C for 6 h, rinsed thoroughly with copious amounts of deionized water and dried under nitrogen. A PAA NMP solution with a composition of 7.3 wt% NMP solvent was spin coated onto a Si wafer (2500 r.p.m. and 90 s). Soft baking was carried

out on a hot plate at 80 °C for 3 min. To achieve identical thermal and dynamic mechanical properties, the content of the resident solvent (ca. 30 wt%) in the PAA films after soft baking was controlled to be the same as that in the PAA thick films.

Fabrication of nanoimprinted PAA films

NIL of the PAA films after soft baking was executed by a commercial nanoimprinter (NM-0401, Meisyo Kiko Co., Ltd., Hyogo, Japan). The imprinting process was carried out in a vacuum to avoid air bubbles. The fabrication process for the nanoimprinted PI film is shown in Scheme 1b. To decrease the adhesion between the polymer and the mold, the Si mold (Kyodo International Inc., Kanagawa, Japan) was treated with Optool DSX (Daikin Industries Ltd., Osaka, Japan; 0.1 wt% in methoxy-nonafluorobutane (HFE7100)) for 1 min, rinsed by HFE7100 and dried under vacuum.

Hard baking process for PAA films

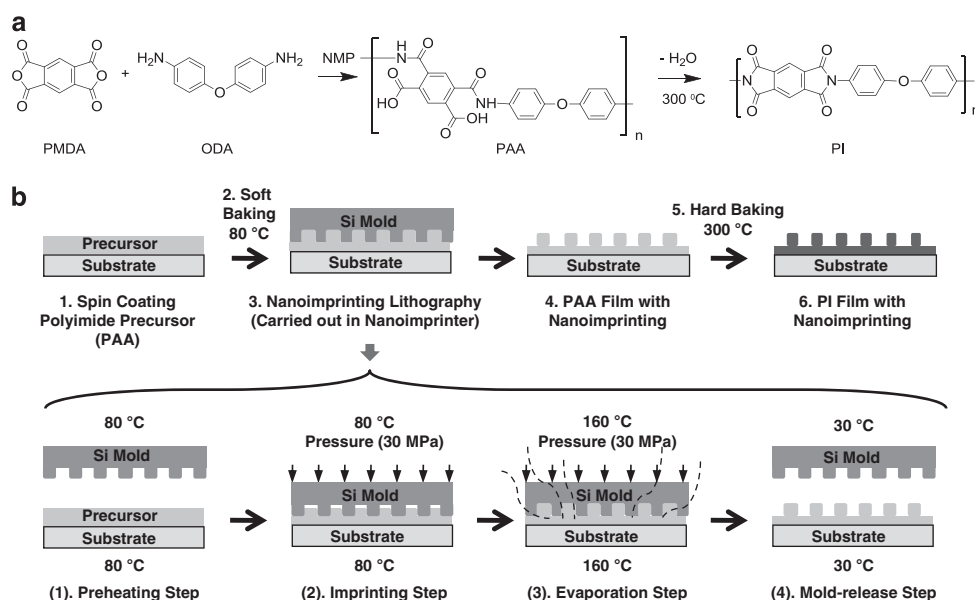
Hard baking was carried out in a muffle furnace (KDF S-70, EYELA, Tokyo, Japan). The thick PI film for the measurement of thermal and dynamic mechanical properties was held between two Si wafers during hard baking to obtain smooth films. The temperature was ramped from room temperature to 300 °C in 1 h, held at 300 °C for 1 h and then cooling down naturally. The thickness of the PI thick film is ca. 58 μm. The same hard baking process was carried out on nanoimprinted PAA films. After hard baking, the thickness of the nanoimprinted PI film measured by AFM was ca. 500 nm.

Characterization

To discuss the thermal and dynamic mechanical properties of PAA thin films used for NIL, DSC, TGA and DMA were carried out on PAA thick films that had been peeled from the substrate and compared with PI films that were obtained through hard baking of PAA thick films.

The DSC curves were obtained using a DSC8230 (Rigaku Co., Ltd., Tokyo, Japan). A 4.1-mg sample for the PAA film and a 4.9-mg sample for the PI film were heated at a heating rate of 10 °C min⁻¹ in an aluminum pan under a nitrogen flow. The samples were cut into a round slice and unfolded on the bottom of the aluminum pan to obtain uniform heating from the sample container.

TGA was examined on an SII Exstar 6000 (TG/DTA 6200, SII. Nano Technology Inc., Chiba, Japan) system between room temperature and 600 °C



Scheme 1 (a) Synthesis of PAA and imidization and (b) fabrication process of nanoimprinted PI films. A full color version of this scheme is available at *Polymer Journal* online.

at a heating rate of $10\text{ }^{\circ}\text{C min}^{-1}$ under nitrogen using the Pt pan. The samples (4.3 mg for PAA and 4.6 mg for PI) were set in the Pt pan using the same method used for the DSC measurement.

DMA was conducted on an Automatic Dynamic Viscoelastomer Rheovibron model DDV-01FP (Orientec A&D Co., Ltd., Tokyo, Japan) at 11 Hz using a heating rate of $3\text{ }^{\circ}\text{C min}^{-1}$. The size of the sample was ca. 3.5 mm wide and ca. 20 mm long.

The effect of hard baking on the topography of the nanoimprinted PI film was studied by AFM (Pacific Nanotechnology, Inc., Nano-RTM, Santa Clara, CA, USA) operating in close-contact mode. Si cantilevers with a 225- μm length, a 2.32-N m^{-1} spring constant and a 73-kHz resonance frequency were used. The scanning rate was 0.1 Hz. To avoid AFM scanning flaws induced by a deep pattern depth, nanoimprinted film with a low depth was prepared, and the same area was observed before and after hard baking. The pitch-width, line-width (L), groove-width (G) and line-height (H) before and after hard baking were discussed through AFM topography images.

RESULTS AND DISCUSSION

Thermal and dynamic mechanical properties of PAA

The DSC curves of the PAA film and the PI film are shown in Figure 1. It is difficult to distinguish the exact T_g of PAA by DSC because it involves information about dehydration with cyclization, evaporation of the residual solvent, depolymerization (chain scission) of PAA and crystallization, which occur simultaneously in some temperature ranges.^{17–20} From the DSC curves of the PAA film, there is a heat flow change at $109\text{ }^{\circ}\text{C}$, which is lower than the starting temperature of the imidization reaction, at ca. $120\text{ }^{\circ}\text{C}$.¹⁷ Although depolymerization (chain scissioning) of PAA¹⁹ and removal of the solvent occur in this temperature range as well, it can be deduced that the T_g of PAA is $\sim 109\text{ }^{\circ}\text{C}$, which agrees with the results reported by

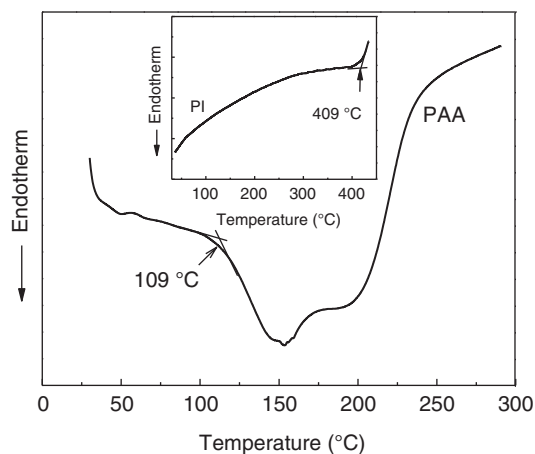


Figure 1 DSC thermograms of a PAA film and a PI film.

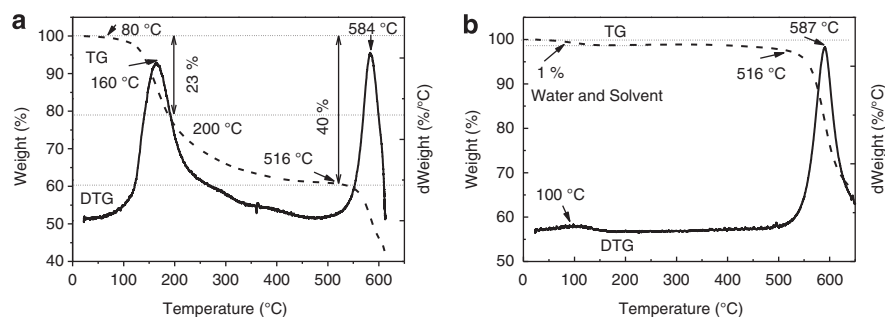


Figure 2 TG and DTG of (a) a PAA film and (b) a PI film.

Nakamae *et al.*²⁰ For comparison, the DSC curve of the PI film is shown in the inset. The T_g of PI is $409\text{ }^{\circ}\text{C}$, which is much higher than that of PAA. Through the DSC analysis, it was confirmed that fabricating nanostructures on PI films directly is unsuitable because of the high T_g of PI.

The thermal stability of PAA films and PI films was evaluated by TGA. From the TGA profile of the PAA film shown in Figure 2a, there are two sharp weight loss events located at $80\text{ }^{\circ}\text{C}$ and $516\text{ }^{\circ}\text{C}$, respectively. In the temperature range $80\text{--}200\text{ }^{\circ}\text{C}$, substantial and rapid weight loss of ca. 23 wt% occurred. This significant weight loss might be because of the removal of the decomplexed NMP solvent and the water given off as a by-product of the imide-ring closures of the PAA polymer chains being imidized.¹⁷ In the range $200\text{--}516\text{ }^{\circ}\text{C}$, the weight loss might result from the removal of the residual solvent and the slow rate of the dehydration of the partially imidized precursor chains. The weight loss at $516\text{ }^{\circ}\text{C}$ shows the initial thermal decomposition temperature of PI. Heating the PAA film from room temperature to $516\text{ }^{\circ}\text{C}$, the weight loss of 40 wt% mainly involves three processes: removal of the solvent (which is ca. 30 wt% in the entire film), dehydration of PAA and evaporation of the small quantity of water that is present in the PAA film. From the DTG profile, the highest rate of weight loss at $160\text{ }^{\circ}\text{C}$ is mainly attributed to the loss of the solvent. The peak at $584\text{ }^{\circ}\text{C}$ indicates the temperature at which the fastest decomposition of PI occurs. Because NIL was performed on the precursor, two points should be noted. First, because the weight loss begins at $80\text{ }^{\circ}\text{C}$, it is better to increase the pressure before excessive removal of the solvent and the imidization reaction. Second, the holding temperature at $160\text{ }^{\circ}\text{C}$ implies partial imidization (ca. 45% imidization has occurred as a result of heating to $160\text{ }^{\circ}\text{C}$.¹⁷) and faster removal of the solvent. In Figure 2b, the PI film exhibits a high thermal stability. At $100\text{ }^{\circ}\text{C}$, a loss of 1 wt% is attributed to the residual water and solvent in the PI film. The initial decomposition temperature of PI is $516\text{ }^{\circ}\text{C}$, and the fastest decomposition was observed at $587\text{ }^{\circ}\text{C}$.

The temperature dependencies of the storage modulus (E'), loss modulus (E'') and $\tan\delta$ of the PAA and PI films, which were measured by using a dynamic forced vibration method at 11 Hz, are shown in Figure 3. From Figure 3a, the PAA film exhibits a minimum storage modulus at $114\text{ }^{\circ}\text{C}$, which might be related to the depolymerization of PAA.¹⁹ After that, the storage modulus increases because the rigidity of the polymer increases with the evaporation of the solvent and the imidization reaction. For the same reason, the loss modulus of the PAA film decreases after the maximum modulus loss at $85\text{ }^{\circ}\text{C}$. In the $\tan\delta$ versus temperature profile, a peak at $97\text{ }^{\circ}\text{C}$ indicates that relaxation occurs, which is assigned to the α_a -absorption of PAA film plasticized by the solvent. After $160\text{ }^{\circ}\text{C}$, the PAA film goes into a dynamically stable state. Consequently, the

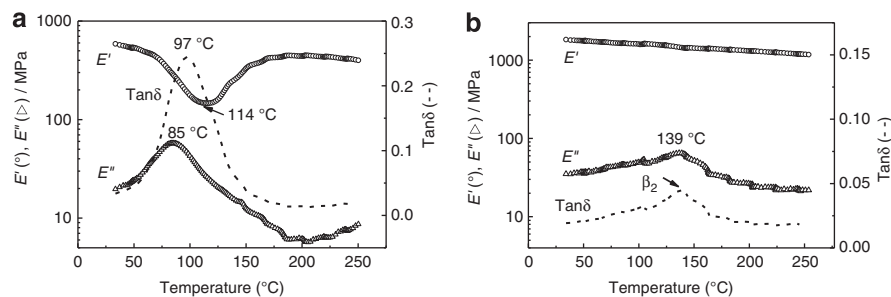


Figure 3 Temperature dependences of the dynamic viscoelasticity for (a) a PAA film and (b) a PI film. Measurements were collected at 11 Hz with an amplitude of 4 μm .

pattern of the film will not be destroyed during the following hard baking process, as long as the dynamic mechanical behavior of the PAA film has been stable. Figure 3b shows the dynamic mechanical properties of the PI film. A slight, steady decrease in E' was observed. The peak in E'' at 139 $^{\circ}\text{C}$ is β_2 absorption, which is attributed to the rotation or oscillations of the phenyl groups within the PI's diamine moiety.²¹ In E'' and the $\tan\delta$ curve, β_2 absorption is associated with a steady decrease in E' . From the $\tan\delta$ curve, α_a -relaxation of PI does not appear below 250 $^{\circ}\text{C}$, indicating that carrying out NIL on PI film directly is not practical for massive fabrication owing to the rigidity of the PI chains.

Soft baking and the nanoimprinting process

Before nanoimprinting, soft baking was conducted on the spin-coated film to partially remove the solvent (NMP). However, the residual solvent should not be completely removed because the rigidity of the chain increases with the evaporation of the solvent and the imidization reaction, leading to an incomplete imprint later. The multiple experiments showed that heating at 80 $^{\circ}\text{C}$ for a few minutes (for example, 3 min) is an appropriate process.

According to the thermal and dynamic mechanical properties of PAA films, an appropriate nanoimprinting process can be designed, and this process is shown in Scheme 1b. The imprinting pressure is <40 MPa to avoid possible mold damage. The most important factors in the process are temperature and time. The first step is the preheating step. The preheating temperature, 80 $^{\circ}\text{C}$, is close to the α_a -absorption of PAA film to protect the Si mold. However, the holding time of this step should not be longer than 1 min to avoid incomplete imprint owing to the loss of solvent. Second step is the imprinting step. Increased pressure (30 MPa) is placed on the Si mold and the sample. According to the thermal and dynamic mechanical properties of PAA films, substantial and rapid weight loss begins at 80 $^{\circ}\text{C}$. With the removal of the solvent and dehydration of PAA, the rigidity of the film will be increased. To provide the polymer with enough time and mobility to flow into the patterned mold, the temperature should be held at 80 $^{\circ}\text{C}$. In this step, the depth of the pattern can be adjusted by altering the holding time. A higher resolution of the pattern can be obtained with a longer holding time. For instance, when the holding times are 10 s and 600 s, patterns with depths of ca. 100 nm and 450 nm (Supplementary Information shows the nanoimprinting process of the nanoimprinted PI films with line-height of ca. 100 nm and 450 nm), respectively, are obtained. Third step is the evaporation step. In this step, the pressure should be maintained. The temperature is increased to 160 $^{\circ}\text{C}$ and maintained for 10 min. This temperature was chosen because a faster evaporation of the solvent occurs at 160 $^{\circ}\text{C}$, as demonstrated with the TG data for

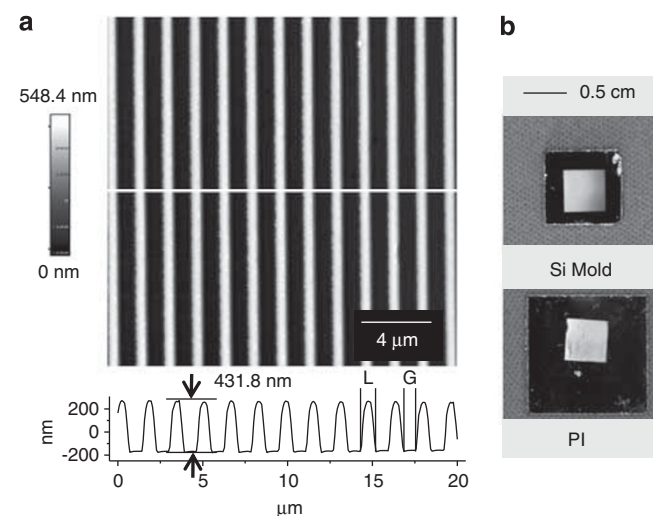


Figure 4 (Color online) (a) AFM image of a nanoimprinted PI film and (b) photos of a Si mold and a nanoimprinted PI film on a Si substrate. L, line-width; G, groove-width. A full color version of this figure is available at *Polymer Journal* online.

the PAA film. By holding the temperature at 160 $^{\circ}\text{C}$ for a certain amount of time (ca. 10 min), the dynamic mechanical properties of the film became stable, which can also be confirmed by TGA and DMA. Therefore, this step is important to keep the pattern undamaged by hard baking. The fourth step is the mold-release step. In the mold-release step, pressure was released after cooling to avoid conglutination, which might happen if the mold were separated from the polymer at a higher temperature.

Effect of hard baking on topography

To achieve stable physical properties for nanoimprinted PI films, the hard baking of a nanoimprinted PAA film was performed at 300 $^{\circ}\text{C}$. Figure 4a shows the topography of the nanoimprinted PI film that was obtained by holding at the imprinting step for 600 s. The H, L and G are 431.8 nm, 941.2 nm and 705.9 nm, respectively. Figure 4b shows photographs of the Si mold and the nanoimprinted PI film on a Si substrate. The relative smoothness and good light reflection indicate that the pattern was successfully transformed. The dynamic mechanical property of the film becomes stable after NIL; thus, distortion of the pattern did not occur, even though a high curing temperature, 300 $^{\circ}\text{C}$, was used.

It is difficult to obtain an accurate AFM image for deeper line patterns, such as those at 400 nm. The cantilever tip cannot easily

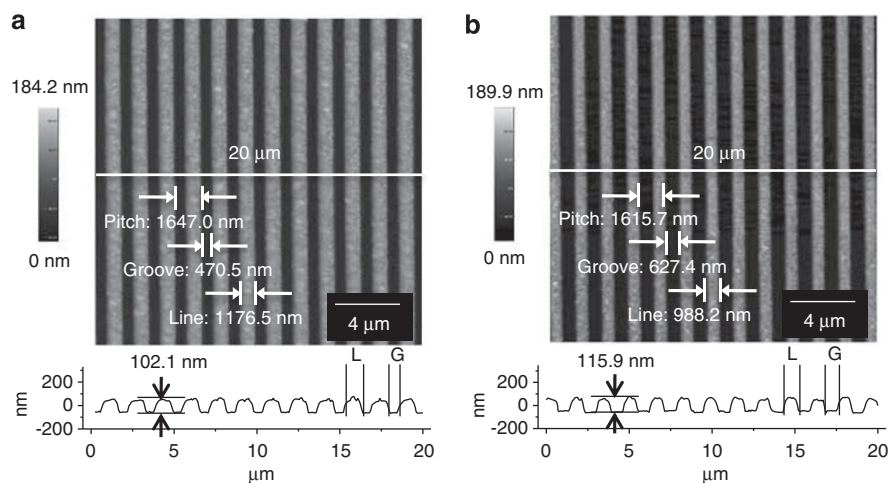


Figure 5 Close-contact-mode AFM images and the corresponding height profiles of (a) a PAA film and (b) a PI film. L, line-width; G, groove-width; Pitch = L + G. A full color version of this figure is available at *Polymer Journal* online.

probe the bottom of the deep grooves. To precisely study the topography of a nanoimprinted film before and after hard baking, a patterned PAA film with imprints of reduced depth was prepared by using a shorter nanoimprinting time, holding at the imprinting step for 10 s. Figures 5a and b show AFM topography images of a PAA film and a PI film, respectively, with line patterns with a depth of ca. 100 nm. The same area was observed by AFM before and after hard baking to avoid the influence of the non-uniformity induced by spin coating or mold deformation. From Figure 5, the uniform shrinkage of lines was observed after hard baking. Figure 5a shows the topography image of the PAA film with an average L of 1176.5 nm, G of 470.5 nm and H of 102.1 nm. After hard baking, the L/G is 988.2 nm/627.4 nm and the H is 115.9 nm (in Figure 5b). The pitch-width (L plus G) has shrunk by ~30 nm, whereas the shrinkage of the L is ~188 nm. The shrinkage of the L causes the G to become 157 nm wider. (Supplementary Information shows the validity analysis of AFM images conducted by a Scanning Probe Image Processor, Nanoscience Instruments, Santa Clara, CA, USA).

During hard baking, the film shrunk because of the evaporation of solvent and the imidization reaction. Because of the presence of hydroxyl groups on the surface of the Si wafer, the carbonyl group in the polymer interacts strongly with the Si wafer, causing the bottom of the film to stretch during the shrinkage process. In contrast, because of the uniform shrinkage of the line, the patterned film was tensioned in the direction perpendicular to the line. From the nanoimprinted PAA film to the nanoimprinted PI film, the shrinkage ratio of the L is 16.0%. The shrinkage ratio of the pitch is 1.8%. It has been reported that a pyromellitic dianhydride/oxydianiline PI film will shrink ca. 20–25% after imidization.²² On the basis of the film thickness of ca. 500 nm and the strong adhesion of the polymer film on the Si substrate, this shrinkage is in a reasonable range. Although there is a remarkable amount of shrinkage induced in the patterned film by hard baking, the shrinkage did not destroy the nanoimprinting, and the well-defined pattern was preserved.

CONCLUSION

NIL was performed on PAA films, which were then cured to obtain patterned PI films. The thermal and dynamic mechanical behavior of PAA films and PI films was investigated. By comparing DSC, TGA and DMA results for PAA films and PI films, we determined that it is

not practical to fabricate nanopatterns on PI films directly, owing to the high thermal stability and rigidity of PI films. Additionally, for PAA films, weight loss starts at 80 °C, and the highest rate of weight loss, at 160 °C, is mainly attributed to the loss of the solvent and the imidization reaction. Furthermore, PAA films enter a dynamically stable state at temperatures > 160 °C. On the basis of the analysis of thermal and dynamic mechanical behavior, an appropriate nanoimprinting condition for PAA films was proposed, which includes four steps: a preheating step, an imprinting step, an evaporation step and a mold-release step. Using this standard process, we have successfully transferred a nanopattern from a Si mold to a PI film. AFM observation of nanoimprinted PAA films and PI films showed a larger shrinkage after hard baking. Although a high curing temperature, such as 300 °C, was used, this shrinkage did not damage the nanopattern because of the optimized nanoimprinting process. Such nanoimprinted PI films have the potential to become an important addition to the field of micro- and nanofabrication.

Supplementary Information: The validity analysis of shrinkage was conducted by a Scanning Probe Image Processor (SPIP). The nanoimprinting process of the nanoimprinted PI films with H of 431 and 100 nm. Supplementary Information is available at the *Polymer Journal*'s website.

ACKNOWLEDGEMENTS

This work was supported by a Grant-in-Aid for the Global COE Program 'Science for Future Molecular Systems' from the Ministry of Education, Culture, Science, Sports and Technology of Japan.

- Mittal, K. L. & Ghosh, M. K. in *Polyimide: Fundamentals and applications* 629–698 (Marcel Dekker, New York, 1996).
- Mittal, K. L. (ed.) *Polyimides: Synthesis, Characterization, and Applications* (Plenum Pub Corp., New York, 1984).
- Song, S., Cho, B., Kim, T. W., Ji, Y., Jo, M., Wang, G., Choe, M., Kahng, Y. H., Hwang, H. & Lee, T Three-dimensional integration of organic resistive memory devices. *Adv. Mater.* **22**, 5048–5052 (2010).
- Chiou, D. R., Yeh, K. Y. & Chen, L. J. Adjustable pretilt angle of nematic 4-n-pentyl-4'-cyanobiphenyl on self-assembled monolayers formed from organosilanes on square-wave grating silica surfaces. *Appl. Phys. Lett.* **88**, 133123 (2006).
- Lin, R. S. & Rogers, J. A. Molecular-scale soft imprint lithography for alignment layers in liquid crystal devices. *Nano Lett.* **7**, 1613–1621 (2007).
- Ree, M High performance polyimides for applications in microelectronics and flat panel displays. *Macromol. Res.* **14**, 1–33 (2006).

- 7 Viventi, J., Kim, D.-H., Vigeland, L., Frechette, E. S., Blanco, J. A., Kim, Y. S., Avrin, A. E., Tiruvadi, V. R., Hwang, S. W., Vanleer, A. C., Wulsin, D. F., Davis, K., Gelber, C. E., Palmer, L., Van der Spiegel, J., Wu, J., Xiao, J., Huang, Y., Contreras, D., Rogers, J. A. & Litt, B. Flexible, foldable, actively multiplexed, high-density electrode array for mapping brain activity in vivo. *Nat. Neurosci.* **14**, 1599–1605 (2011).
- 8 Nie, Z. & Kumacheva, E. Patterning surfaces with functional polymers. *Nat. Mater.* **7**, 277–290 (2008).
- 9 Lee, B. W. & Clark, N. A. Alignment of liquid crystals with patterned isotropic surfaces. *Science* **291**, 2576–2580 (2001).
- 10 Thibault, C., Molnar, G., Salmon, L., Bousseksou, A. & Vieu, C. Soft lithographic patterning of spin crossover nanoparticle. *Langmuir* **26**, 1557–1560 (2010).
- 11 Krämer, S., Fuierer, R. R. & Gorman, C. B. Scanning probe lithography using self-assembled monolayers. *Chem. Rev.* **103**, 4367–4418 (2003).
- 12 Akiyama, H., Momose, M., Ichimura, K. & Yamamura, S. Surface-selective modification of poly(vinyl alcohol) films with azobenzenes for inplane alignment photocontrol of nematic liquid-crystals. *Macromolecules* **28**, 288–293 (1995).
- 13 Honda, K., Morita, M. & Takahara, A. Room-temperature fabrication of nanotexture in crystalline poly(fluoroalkyl acrylate) thin film. *Soft Matter* **4**, 1400–1402 (2008).
- 14 Chou, S. Y., Krauss, P. R. & Renstrom, P. J. Imprint of Sub-25 Nm vias and trenches in polymers. *Appl. Phys. Lett.* **67**, 3114–3116 (1995).
- 15 Ofir, Y., Moran, I. W., Subramani, C., Carter, K. R. & Rotello, V. M. Nanoimprint lithography for functional three-dimensional patterns. *Adv. Mater.* **22**, 3608–3614 (2010).
- 16 Cui, B., Cortot, Y. & Veres, T. Polyimide nanostructures fabricated by nanoimprint lithography and its applications. *Microelectron. Eng.* **83**, 906–909 (2006).
- 17 Shin, T. J., Lee, B., Youn, H. S., Lee, K.-B. & Ree, M. Time-resolved synchrotron X-ray diffraction and infrared spectroscopic studies of imidization and structural evolution in a microscaled film of PMDA-3,4'-ODA poly(amic acid). *Langmuir* **17**, 7842–7850 (2001).
- 18 Snyder, R. W., Thomson, B., Bartges, B., Czerniawski, D. & Painter, P. C. FTIR studies of polyimides: thermal curing. *Macromolecules* **22**, 4166–4172 (1989).
- 19 Ando, S., Matsuura, T. & Nishi, S. ¹³C NMR analysis of fluorinated polyimides and poly(amic acids). *Polymer* **33**, 2934–2939 (1992).
- 20 Kotera, M., Nishino, T. & Nakamae, K. Imidization processes of aromatic polyimide by temperature modulated DSC. *Polymer* **41**, 3615–3619 (2000).
- 21 Chern, Y.-T. Low dielectric constant polyimides derived from novel 1,6-Bis[4-(4-aminophenoxy)phenyl]diamantane. *Macromolecules* **31**, 5837–5844 (1998).
- 22 Wang, Y. W., Yen, C. T. & Chen, W. C. Photosensitive polyimide/silica hybrid optical materials: synthesis, properties, and patterning. *Polymer* **46**, 6959–6967 (2005).

Supplementary Information accompanies the paper on Polymer Journal website (<http://www.nature.com/pj>)